

Gastrointestinal, Hepatobiliary and Pancreatic Pathology

Oncostatin M Inhibits Proliferation of Rat Oval Cells, OC15-5, Inducing Differentiation into Hepatocytes

Atsuhito Okaya,^{*†} Junichi Kitanaka,[‡]
Nobue Kitanaka,[‡] Makoto Satake,^{*†} Yuna Kim,^{*}
Kunihiko Terada,[§] Toshihiro Sugiyama,[§]
Motohiko Takemura,[‡] Jiro Fujimoto,[†]
Nobuyuki Terada,^{*} Atsushi Miyajima,[¶] and
and Tohru Tsujimura^{*}

From the Departments of Pathology,^{*} Surgery,[†] and
Pharmacology,[‡] Hyogo College of Medicine, Hyogo; the
Department of Biochemistry,[§] Akita University School of
Medicine, Akita; and the Institute of Molecular and Cellular
Biosciences,[¶] University of Tokyo, Tokyo, Japan

Oval cells of the liver participate in liver regeneration when hepatocytes are prevented from proliferating in response to liver damage. To clarify the role of oncostatin M (OSM) in the liver regeneration involving oval cells, we examined the expression of OSM and OSM-specific receptor (OSM-R) in the liver undergoing regeneration in the 2-acetylaminofluorene/partial hepatectomy model. Expression levels of OSM-R changed in correlation to the number of oval cells, and its expression was exclusively observed in oval cells. On the other hand, OSM was expressed in both oval cells and Kupffer cells. To examine the effect of OSM on the growth and differentiation of oval cells, rat oval cells (OC15-5) were incubated in conditioned medium of 293T cells expressing rat OSM cDNA. This resulted in suppression of growth, changes in morphology (microvilli and large cytoplasm with developed organelles), and expression of hepatocyte markers (albumin, tyrosine amino transferase, and tryptophan oxygenase). The effects of the conditioned medium with rat OSM were abrogated by introducing a small interfering RNA specifically targeting rat OSM-R into OC15-5 cells. These results indicate that OSM is a key mediator for inducing differentiation of OC15-5 cells into hepatocytes and suggest that the OSM/OSM-R system is pivotal in the differentiation of oval cells into hepatocytes, thereby promoting liver regeneration. (*Am J Pathol* 2005, 166:709–719)

In acute liver injury, hepatocytes rapidly proliferate to repair the damage.^{1–3} Hepatic stem/progenitor cells usu-

ally do not take part in such acute liver regeneration. However, when hepatocytes are prevented from proliferating in response to liver damage, oval cells, characterized by ovoid nucleus, small in cellular size, and a high nuclear-to-cytoplasmic ratio, emerge from the canal of Hering and proliferate in the periportal areas.^{2–8} For example, in the rat 2-acetylaminofluorene/partial hepatectomy (AAF/PH) model, in which hepatocyte proliferation is inhibited by AAF administration, PH initiates the generation of numerous oval cells.⁹ Oval cells express albumin and, in addition, exhibit features of fetal hepatocytes and bile epithelial cells, expressing α -fetoprotein (AFP) and cytokeratin (CK)-19, respectively.⁵ They also share characteristics with hematopoietic stem cells, expressing *c-kit* receptor tyrosine kinase, CD34, and Thy-1.^{10–13} Oval cells are presumed to be hepatic progenitors in the adult liver and participate in the liver regeneration when the replicative and functional capacity of hepatocytes is impaired.^{2,3,5–8} However, the molecular mechanism underlying the differentiation of oval cells into hepatocytes remains to be established.

Oncostatin M (OSM) is a member of the interleukin-6 cytokine family that includes interleukin-6, interleukin-11, leukemia inhibitory factor, ciliary neurotrophic factor, cardiotrophin-1, and novel neutrophin-1/B-cell-stimulating factor-3.^{14–16} Mouse OSM receptor is composed of the gp130 subunit, common to all of the interleukin-6 family cytokines,¹⁵ and the OSM-specific subunit¹⁷ (hereafter this subunit is called OSM-specific receptor: OSM-R). Ligand binding to the receptor complex activates the Janus tyrosine kinases (Jak1, Jak2, and Tyk2) and the activated Jaks in turn activate downstream pathways, such as SHP-2 tyrosine phosphatase and signal transducer and activator of transcription protein 3.¹⁵ Recently, OSM has been shown to induce maturation of mouse fetal hepatocytes derived from the embryonic day 14.5 liver as characterized by the expression of tyrosine amino trans-

Supported in part by Grants-in-Aid for Scientific Research from the Ministry of Education, Science, Sports, and Culture of Japan and for graduate students, Hyogo College of Medicine.

Accepted for publication November 30, 2004.

Address reprint requests to Tohru Tsujimura, M.D., Ph.D., Department of Pathology, Hyogo College of Medicine, 1-1, Mukogawa, Nishinomiya, Hyogo 663-8501, Japan. E-mail: tohru@hyo-med.ac.jp.

Table 1. Oligonucleotide Primers Used for Determination of Rat *OSM-R* and *OSM* cDNA Sequences

Oligonucleotide	Sequence	Position
rFW1	5'-CCCCTGTGAGGCCGAGGACCGGC-3'	34-56*
rFW2	5'-TGGAAGAAGGCTCCAATGTCACCAT-3'	565-589*
rFW3	5'-TGCCAACCACTTCTGGAAATGGAG-3'	1310-1333*
rFW4	5'-TTCTGGGAGCCGGTATCTGGAGAC-3' [†]	1721-1745*
rFW5	5'-GTGCCAACAGAAAAGGATTCTC-3'	2595-2617*
rFW6	5'-CCCTGGTCGAAAGTCCAAGTGAAGA-3'	2788-2812*
rRV1	5'-TGGCTTTACAATTGATGTTTGTCCCTG-3' [†]	718-744*
rRV2	5'-CTCCACACATCAAGAGCTTCTGAG-3' [†]	1376-1399*
rRV3	5'-CACACCAGTCCACAACATAGCC-3'	1752-1773*
rRV4	5'-CCATTTGCCTTTTATACTCTGAAC-3'	2902-2925*
slica1	5'-CAATTAACCCTCACTAAAGA-3'	
slica2	5'-CTAAAGAATTCAAGTCAGTCA-3'	
FW1	5'-GGCACGGGCCAGAGTACCAGGACCCAG-3'	14-40 [‡]
FW2	5'-GTGGCCTTCCCCAGTGAGGA-3'	267-286 [‡]
FW3	5'-CCTGAGCCCACACAGGCAGACTCTGGG-3' [‡]	492-518 [‡]
FW4	5'-TCTTTCAGATCAAGATAGACAGCTG-3' [‡]	547-571 [‡]
RV1	5'-GTGGCGTGCACAGTGCTCAGGAAGT-3' [‡]	313-337 [‡]
RV2	5'-CCCCACTGAGCCCATGAAGCGATGGTA-3'	588-614 [‡]

*Number of the mouse *OSM-R* cDNA (GenBank accession number AF058805).

[†]Based on rat *OSM-R* cDNA sequence described in this study.

[‡]Number of the mouse *OSM* cDNA (GenBank accession number D31942).

[‡]Based on rat *OSM* cDNA sequence described in this study.

ferase (TAT) and glucose-6-phosphatase, which are expressed in the perinatal liver, and the accumulation of glycogen.¹⁸ OSM in combination with extracellular matrices derived from Engelbreth-Holm-Swarm sarcoma has also been shown to induce tryptophan oxygenase (TO), a liver-specific enzyme expressed by fully matured hepatocytes, in mouse fetal hepatocytes.¹⁹ In addition, human fetal hepatocytes, like mouse fetal hepatocytes, have been reported to be induced to differentiate by OSM.²⁰ These results indicate that OSM is a crucial factor for liver development involving maturation of fetal hepatocytes. Because oval cells, like fetal hepatocytes, are believed to represent hepatic progenitors, there is a possibility that OSM may play an important role in liver regeneration involving differentiation of oval cells. To investigate this possibility, we isolated rat *OSM-R* and *OSM* cDNA and examined whether OSM induces the differentiation of rat oval cells, OC15-5, into hepatocytes.

Materials and Methods

Rats and Treatments

Oval cells were induced in male Fischer 344 rats of 6 weeks of age (SLC, Hamamatsu, Japan) by the method of the AAF/PH model.¹¹ Briefly, AAF (Wako Pure Chemical Industries, Ltd., Osaka, Japan) was daily administered to rats by gavage at 10 mg/kg body weight for 4 days. On day 5, a standard two-thirds PH was performed, and then the daily administration of AAF at the same dosage continued for 5 days. All animal studies were performed in accordance with the criteria outlined in the Guide for the Care and Use of Laboratory Animals prepared by the National Academy of Science.

Preparation of Parenchymal and Nonparenchymal Cells

Parenchymal and nonparenchymal cells of the liver were isolated by the two-step collagenase digestion method with some modifications, as previously described.²¹

Isolation of Rat *OSM-R* and *OSM* cDNA

To obtain rat *OSM-R* cDNA, RNA was prepared from the liver on day 7 after PH in the AAF/PH model using TRIzol reagent (Life Technologies, Inc., Grand Island, NY), reverse-transcribed by Superscript II reverse transcriptase (RT) (Life Technologies, Inc.) and an anchor primer (5'-GCAATTAACCCTCACTAAAGAATTCAAGTCAGTCA(T)₁₇-3'), and amplified by polymerase chain reaction (PCR) using *Taq* Ex (Takara Shuzou, Kyoto, Japan) and four sets of primers (rFW1 and rRV1, rFW2 and rRV2, rFW3 and rRV3, and rFW4 and rRV4) (Table 1) with 25 cycles of 94°C for 30 seconds, 58°C for 30 seconds, and 72°C for 1 minute. Nested PCR was performed using rFW5 and slica1 as the first set of primers and rFW6 and slica2 as the second set of primers (Table 1) to obtain the 3'-end of rat *OSM-R* cDNA. To obtain rat *OSM* cDNA, RNA was similarly prepared from the fetal liver on embryonic day 14.5, reverse-transcribed, and amplified by PCR using *Taq* Ex and two sets of primers (FW1 and RV1 and FW2 and RV2) (Table 1). Nested PCR was performed using FW3 and slica1 as the first set of primers and FW4 and slica2 as the second set of primers (Table 1) to obtain the 3'-end of rat *OSM* cDNA. The products were subcloned into the *EcoRV* site of Bluescript I KS(-) (Stratagene, La Jolla, CA), and analyzed for nucleotide sequences.

Northern Blot Analysis

Northern blot analysis was performed as previously described.²¹ ³²P-labeled rat *OSM-R* and *glyceraldehyde-3-phosphate dehydrogenase* cDNA were used as probes. Analysis of *OSM-R* and *OSM* mRNA in various tissues was conducted using a membrane of rat poly A⁺ RNA (2 μg) Northern blot-12 major tissues (OriGene Technologies, Inc., Rockville, MD) and the *OSM-R* and *OSM* probes.

Number of Oval Cells

Liver tissues were fixed with methacarn, embedded in paraffin, and cut into 5-μm-thick sections. The sections were immunostained with mouse anti-human CK-19 antibody (Novocastra Laboratories, Ltd., Newcastle, UK) diluted 1:40. The number of CK-19-positive oval cells was counted in 10 periportal fields selected randomly in each CK-19-immunostained specimen and expressed as the number per periportal field.

In Situ Hybridization

Liver tissues were fixed with 4% paraformaldehyde, embedded in paraffin, and cut into 5-μm-thick sections. One section was used for *in situ* hybridization and the adjacent section was stained with hematoxylin and eosin. Complementary RNA probes of *OSM-R* were prepared by using a DIG RNA labeling kit (Roche Diagnostics GmbH, Mannheim, Germany). Signals were visualized with a DAKO Gen Point kit (DAKO, Glostrup, Denmark) using the horseradish peroxidase-conjugated anti-digoxigenin antibody (DAKO).

Confocal Laser-Scanning Microscope

For double staining for *OSM-R* and CK-19, nonparenchymal cells were prepared from the liver on day 7 after PH in the AAF/PH model, cytocentrifuged, and fixed with methacarn. For double staining for *OSM* and CK-19 and that for *OSM* and ED2, liver tissues on day 7 after PH in the AAF/PH model were fixed with methacarn, embedded in paraffin, and cut into 5-μm-thick sections. The cytocentrifuged specimens and liver sections were incubated with goat anti-mouse *OSM-R* antibody (R&D Systems, Minneapolis, MN) diluted 1:50 or goat anti-mouse *OSM* antibody (R&D Systems) diluted 1:50 at 4°C overnight. Then, they were sequentially incubated with biotin-conjugated donkey anti-goat IgG antibody (Santa Cruz Biotechnology, Santa Cruz, CA) diluted 1:200 for 60 minutes, horseradish peroxidase-conjugated streptavidin diluted 1:100 for 30 minutes, biotiny tyramine diluted 1:50 for 10 minutes, and fluorescein isothiocyanate-conjugated streptavidin (DAKO) diluted 1:40 for 30 minutes. After washing, the cytocentrifuged specimens were incubated with mouse anti-human CK-19 antibody diluted 1:40, and the liver sections were incubated with mouse anti-human CK-19 antibody diluted 1:40 or mouse anti-rat ED2 antibody (Serotec Ltd., Oxford, UK) diluted 1:500 for 60

minutes. They were then incubated with R-phycoerythrin-conjugated goat anti-mouse IgG (DAKO) diluted 1:100 for 60 minutes. Co-localization of fluorescein isothiocyanate and R-phycoerythrin was analyzed with a confocal laser-scanning microscope (LSM510; Carl Zeiss Jena GmbH, Jena, Germany).

Flow Cytometry

Cells were incubated with rabbit anti-c-kit antibody (Santa Cruz), rabbit anti-CD34 antibody (Santa Cruz), rabbit anti-Thy-1 antibody (Santa Cruz), or goat anti-*OSM-R* antibody at 4°C for 30 minutes. After washing, cells were incubated with biotin-conjugated anti-rabbit IgG antibody (Santa Cruz) or biotin-conjugated anti-goat IgG antibody (Santa Cruz). Cells were then stained with R-phycoerythrin-streptavidin (BD PharMingen, San Diego, CA) and analyzed on a FACSCalibur (Becton Dickinson, Los Angeles, CA). All antibodies used were diluted 1:100.

Preparation of Full-Length Rat *OSM* cDNA and Conditioned Media

The entire coding region of rat *OSM* cDNA was generated by RT-PCR with a set of 5'-ATGCGGGCTCAGCCTCCACCGAGAA-3' and 5'-TTACCGGGGCACCAGG-GACCTGAGCATG-3' primers and was subcloned into the expression vector pEF-BOS. The pEF-BOS DNA with or without rat *OSM* cDNA (10 μg) was transfected into 293T cells by the calcium phosphate method.²² Transfectants with the pEF-BOS DNA with or without rat *OSM* cDNA were cultured in Dulbecco's modification of Eagle's medium (ICN Biomedicals Inc., Aurora, OH) supplemented with 10% fetal bovine serum (HyClone, Logan, UT) for 2 days, and the media were used as the conditioned medium with *OSM* or without *OSM*, respectively. The medium, in which 293T cells treated with calcium phosphate without pEF-BOS DNA were grown for 2 days, was used as the control conditioned medium.

Treatment of OC15-5 Cells with Conditioned Media

OC15-5 cells were plated at a density of 1 × 10⁵ per 100-mm dish and incubated in Dulbecco's modification of Eagle's medium supplemented with 10% fetal bovine serum at 37°C for 24 hours. An equal amount of conditioned medium was added to the culture, and incubation continued for 4 days. Viable OC15-5 cells were determined by the trypan blue exclusion method.

Electron Microscopy

Cells were fixed in 2.5% glutaraldehyde and 1% osmium tetroxide, dehydrated in a graded series of ethanol, and embedded in epoxy resin. Ultrathin sections were stained with uranyl acetate and lead citrate, and examined with a JEM-1220 electron microscope (JEOL, Tokyo, Japan).

Table 2. Oligonucleotide Primers Used for RT-PCR of Liver-Specific Genes

Gene name	Sequence	Product size	GenBank accession no.
CK-19	5'-CGACTGGTACCAGAAGCAGG-3' 5'-GCAGCTTTCATGCTGAGCTG-3'	619bp	X81449
AFP	5'-AACAGCAGACTGCTGCAAAC-3' 5'-TGATGCAGAGCCTCCTGTTG-3'	644bp	X02361
Albumin	5'-ATACACCCAGAAAGCACCTC-3' 5'-CAGAGTGAAGGTGAAGGTC-3'	305bp	V01222
TAT	5'-GGGAGGAGGTCGCTTCTTAC-3' 5'-GGAACATTGGTGCTGAGGTT-3'	457bp	M18340
TO	5'-AACGCACACCTGGCTTAGAG-3' 5'-CTTGCTGCCTAGCATCCTGT-3'	389bp	M55167
GAPDH	5'-ATCACTGCCACTCAGAAGAC-3' 5'-TGAGGGAGATGCTCAGTGTT-3'	578bp	X02231

GAPDH, glyceraldehyde-3-phosphate dehydrogenase.

RT-PCR

Total RNA was reverse-transcribed by Superscript II RT in the presence of random hexamers, and the resultant cDNA was amplified using *Taq* Ex and a set of sense and anti-sense primers (Table 2) by 30 cycles of 94°C for 30 seconds, 60°C for 30 seconds, and 72°C for 1 minute. PCR products were analyzed by electrophoresis in 1.0% agarose gel containing ethidium bromide.

Western Blot Analysis

Cells were lysed in RIPA buffer (10 mmol/L Tris-HCl, pH 7.2, 150 mmol/L NaCl, 1 mmol/L *O,O'*-bis(2-aminoethyl) ethylene glycol-*N,N,N',N'*-tetraacetic acid, 1% Triton X-100, 1% sodium deoxycholate, 0.1% sodium dodecylsulfate, 1 mmol/L phenylmethyl sulfonyl fluoride, 10 mg/ml leupeptin, and 10 mg/ml aprotinin) on ice for 30 minutes and centrifuged at 15,000 × *g* for 30 minutes. The supernatant was subjected to sodium dodecylsulfate-10% polyacrylamide gel electrophoresis. After electrophoresis, proteins were electrophoretically transferred onto a nitrocellulose transfer membrane (Nitrobind; Micron Separations, Inc., Westborough, MA). Immunoblotting was then performed with mouse monoclonal antibody against CK-19 (Progen Biotechnik GmbH, Heidelberg, Germany) or rabbit polyclonal antibody against rat albumin (ICN Pharmaceuticals, Inc., Aurora, OH).

Small Interfering RNA (siRNA) and Transfection

To construct a vector expressing siRNA for rat *OSM-R*, annealed oligonucleotides (5'-ggatcccgTTATGAGTGAT-AGGATGCTGCTgtatgccgGCAGCATCCTATCACTCAT-AAttttttccaaaagctt-3') (*OSM-R* target sequence in capital letters) were subcloned into pRNAT-U6.1/Neo, an siRNA expression vector (GenScript Corp., Piscataway, NJ). The resultant plasmid was designated pRNAT-U6.1/Neo-*OSM-R*. pRNAT-U6.1/Neo or pRNAT-U6.1/Neo-*OSM-R* (10 μg) was transferred into OC15-5 cells (1 × 10⁷) by electroporation (975 mF, 350 V) using Gene Pulser II (Bio-Rad Laboratories, Hercules, CA). Two days after the electroporation, 400 μg/ml of G418 sulfate (geneticin; Life Technologies, Inc.) was added to the culture medium to obtain neomycin-resistant cells.

Statistical Analysis

Statistical analysis was performed by unpaired, two-tailed Student's *t*-test. A *P* value less than 0.05 was considered significant.

Results

Isolation of Rat *OSM-R* cDNA

Human and mouse *OSM-R* cDNA were previously isolated,^{17,23} but rat *OSM-R* cDNA was not. To examine the expression of *OSM-R* mRNA in rat oval cells, we attempted to isolate rat *OSM-R* cDNA. Four overlapping fragments covering most of the *OSM-R* cDNA were obtained by RT-PCR using the liver RNA on day 7 after PH in the AAF/PH model. The 3'-portion of *OSM-R* cDNA was obtained by nested PCR using two sets of primers, rFW5-slica1 and rFW6-slica2 (Figure 1A). The coding region of rat *OSM-R* gene showed 89% and 71% homologies to the mouse and human counterparts, respectively.^{17,23} Analysis of *OSM-R* mRNA in various tissues revealed that *OSM-R* mRNA was expressed in all tissues examined, with the liver, skin, and spleen showing strong signals (Figure 2).

Expression of *OSM-R*

We examined whether the level of *OSM-R* mRNA was correlated with the number of oval cells developed in the AAF/PH model. As shown in Figure 3A, the number of CK-19-positive oval cells increased rapidly for 7 days after PH and then gradually decreased. Northern blot analysis showed that *OSM-R* mRNA was hardly detectable on day 0, but was expressed from day 4 to day 13 after PH. (Figure 3B). These results indicate that the level of *OSM-R* mRNA changed with the number of oval cells.

It has been shown that oval cells are present in the nonparenchymal cell fraction, but not in the parenchymal cell fraction.²¹ Northern blot analysis showed that a strong signal of *OSM-R* mRNA was observed in nonparenchymal cells isolated from the livers on day 7, whereas it was hardly detectable in parenchymal cells isolated from the same livers (Figure 3B). We performed *in situ* hybridiza-

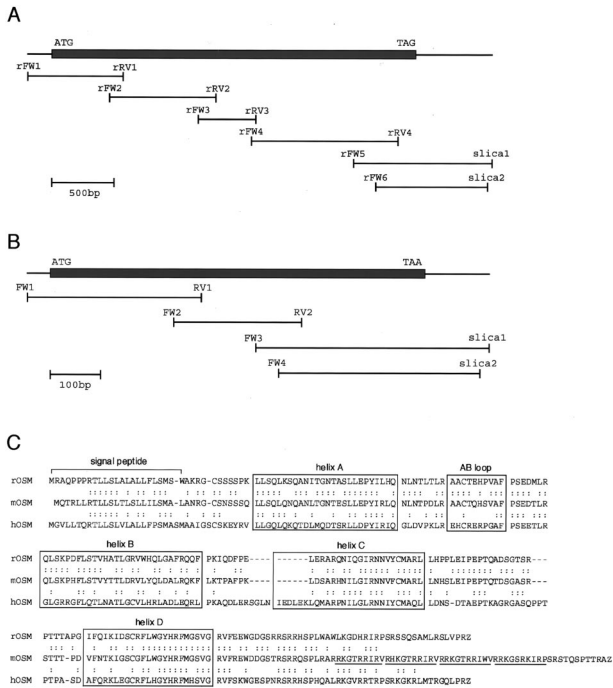


Figure 1. Rat *OSM-R* and *OSM* cDNA. **A:** Schematic representation of rat *OSM-R* cDNA. An open reading frame of rat *OSM-R* cDNA is indicated by shaded box. Six overlapping partial clones are shown below with primers. The sequence of the entire coding region of rat *OSM-R* cDNA encoding a 962-amino acid protein was registered in GenBank under accession no. AB167522. **B:** Schematic representation of rat *OSM* cDNA. An open reading frame of rat *OSM* cDNA is indicated by shaded box. Four overlapping partial clones are shown below with primers. The sequence of the entire coding region of rat *OSM* cDNA encoding a 239-amino acid protein was registered in GenBank under accession no. AB1667521. **C:** Sequence alignment of rat, mouse, and human OSM. Identical amino acids between rat and mouse OSM or between mouse and human OSM were indicated by a :. The predicted helices, signal peptides, and AB loops are also shown. Four repeats present in the C-terminal of mouse OSM, but not rat and human OSM, are indicated by underlines.

tion analysis to identify the type of cells expressing *OSM-R* mRNA in the liver on day 7 after PH. Signals of *OSM-R* mRNA were observed in oval cells that were present at the periportal field and the surrounding parenchyma (Figure 3, C and D). Furthermore, immunohistochemical double-staining analysis of CK-19 and *OSM-R* in nonparenchymal cells isolated from the livers on day 7 after PH showed that CK-19-positive oval cells were also positive for *OSM-R* protein (Figure 3; E to G).

Expression of OSM

RT-PCR analysis showed the expression of OSM in the livers on days 7, 9, 11, and 13 after PH, when numerous oval cells were generated (data not shown). Because these results suggested that oval cells express OSM as well as *OSM-R*, we performed immunohistochemical double-staining analysis of CK-19 and OSM in the liver on day 7 after PH. Oval cells positive for CK-19 were found to be positive for OSM (Figure 4; A to C). Recently, Kupffer cells were shown to be a major source of OSM in the mouse liver injured by the administration of carbon tetrachloride.²⁴ So, we performed immunohistochemical double-staining analysis of ED2, a marker of Kupffer

cells, and OSM in the liver on day 7. Kupffer cells identified by ED2 expression were positive for OSM protein (Figure 4; D to F).

Isolation of Rat OSM cDNA

Human and mouse *OSM* cDNA were previously isolated,^{25,26} but rat *OSM* cDNA was not. To clarify the effect of OSM on rat oval cells, we isolated rat *OSM* cDNA. Two overlapping fragments covering approximately two thirds of *OSM* cDNA from the 5'-end were obtained by RT-PCR using the liver RNA from 14.5-day rat embryos. The 3'-portion of *OSM* cDNA was obtained by nested PCR using two sets of primers, FW3-slica1 and FW4-slica2 (Figure 1B). The coding region of rat *OSM* gene showed 81% and 53% homologies to the mouse and human counterparts, respectively.^{25,26} *OSM* mRNA was found to be expressed in the spleen, thymus, and lung, but not other tissues (Figure 2).

Establishment of the Rat Oval Cell Line OC 15-5

Long-Evans Cinnamon rats carry a defect in the *Wilson disease* gene, resulting in the accumulation of copper in the liver. Long-Evans Cinnamon rats suffer from acute hepatitis at ~4 months of age, and survivors develop chronic hepatitis with the generation of numerous oval cells.²⁷ We isolated these oval cells and cultured for a long time to establish a cell line, designated as OC15-5. OC15-5 cells grew with a cobblestone appearance (Figure 5A) and expressed *CK-19*, *AFP*, and *albumin* mRNA as detected by RT-PCR analysis (Figure 5B). These cells were also positive for *c-kit* receptor tyrosine kinase, *CD34*, and *Thy-1*, which were new surface markers of oval cells,¹⁰⁻¹³ and *OSM-R* (Figure 5C).

Effect of OSM on OC15-5 Cells

The effect of OSM on OC15-5 cells was examined using the conditioned medium of 293T cells transfected with the pEF-BOS with or without rat *OSM* cDNA. Medium, in which 293T cells treated with calcium phosphate without pEF-BOS DNA were grown, was used as the control

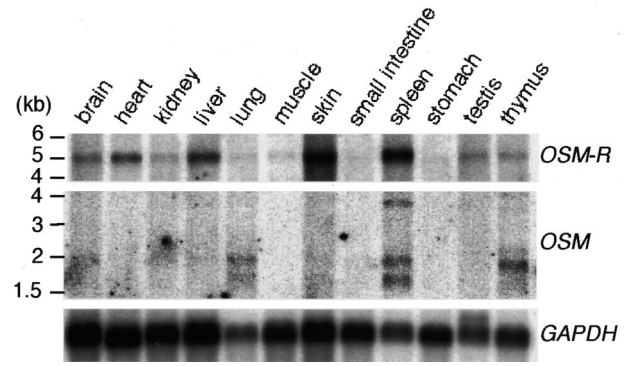


Figure 2. Expression of *OSM-R* and *OSM* mRNA in various adult rat tissues. A membrane of rat poly A⁺ RNA (2 μg) Northern blot-12 major tissues was used for Northern blot analysis. *Glyceraldehyde-3-phosphate dehydrogenase* (*GAPDH*) mRNA was analyzed as an internal standard.

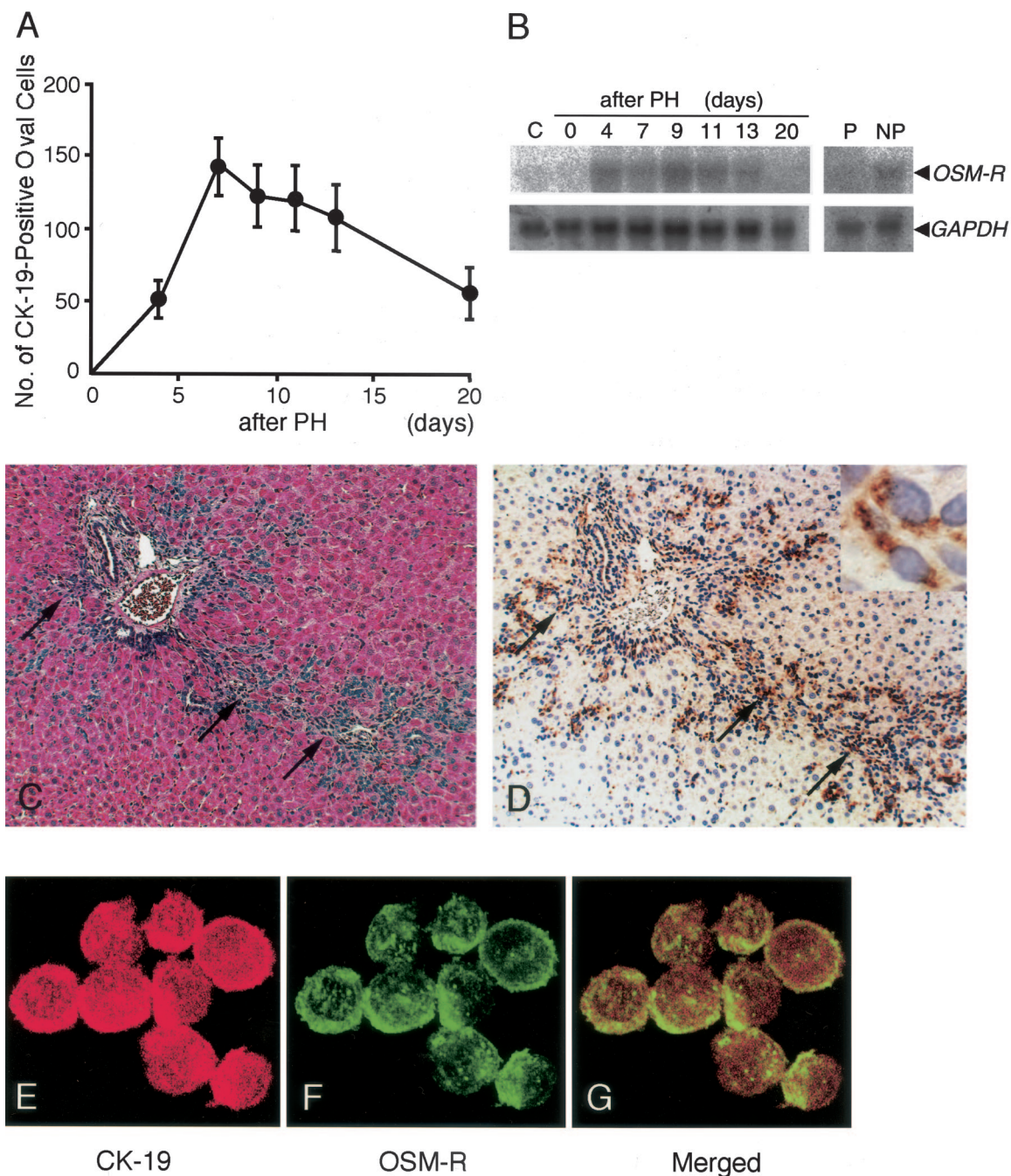


Figure 3. Expression of OSM-R in oval cells. **A:** Time-course analysis of CK-19-positive oval cells in rat livers after PH in the AAF/PH model. Rats were sacrificed on the indicated days after PH, and liver sections were immunostained with anti-CK-19 antibody. The number of CK-19-positive oval cells was counted in 10 periportal fields, and its value was expressed as the number per periportal field (0.25 mm × 0.25 mm). Each point represents the mean of three rats. Bars are standard errors. **B:** Time-course analysis of *OSM-R* mRNA in rat livers after PH in the AAF/PH model. Total liver RNA (20 μg) from rats sacrificed on the indicated days after PH was analyzed by Northern blotting. RNA from rats that did not undergo AAF/PH treatment was used as the control (C). Parenchymal cell fraction (P) and nonparenchymal cell fraction (NP) were isolated from livers on day 7 after PH, and total RNA (20 μg) was analyzed by Northern blotting. *Glyceraldehyde-3-phosphate dehydrogenase (GAPDH)* mRNA was analyzed as an internal standard. **C:** A section of the liver obtained on day 7 after PH stained with H&E. The representative clusters of oval cells are shown by arrows. **D:** *In situ* hybridization analysis of *OSM-R* mRNA using an adjacent section of **C**. Inset in **D** is high magnification and shows oval cells expressing *OSM-R* mRNA. **E:** Fluorescein for CK-19, which is a marker of oval cells (red). **F:** Fluorescein for OSM-R (green). **G:** Merged confocal image of **E** and **F**. **E** to **G** are the photographs, demonstrated by confocal laser-scanning microscopy, of the same cytocentrifuged specimen. Original magnifications: ×90 (**C**, **D**); ×800 (inset in **D**).

conditioned medium. We first examined the effect of OSM on the growth of OC15-5 cells. OC15-5 cells cultured with the conditioned medium without OSM markedly proliferated as cells cultured with the control conditioned me-

dium. In contrast, OC15-5 cells cultured with the conditioned medium with OSM grew poorly (Figure 6).

We next examined the effect of OSM on the differentiation of OC15-5 cells. OC15-5 cells cultured with the

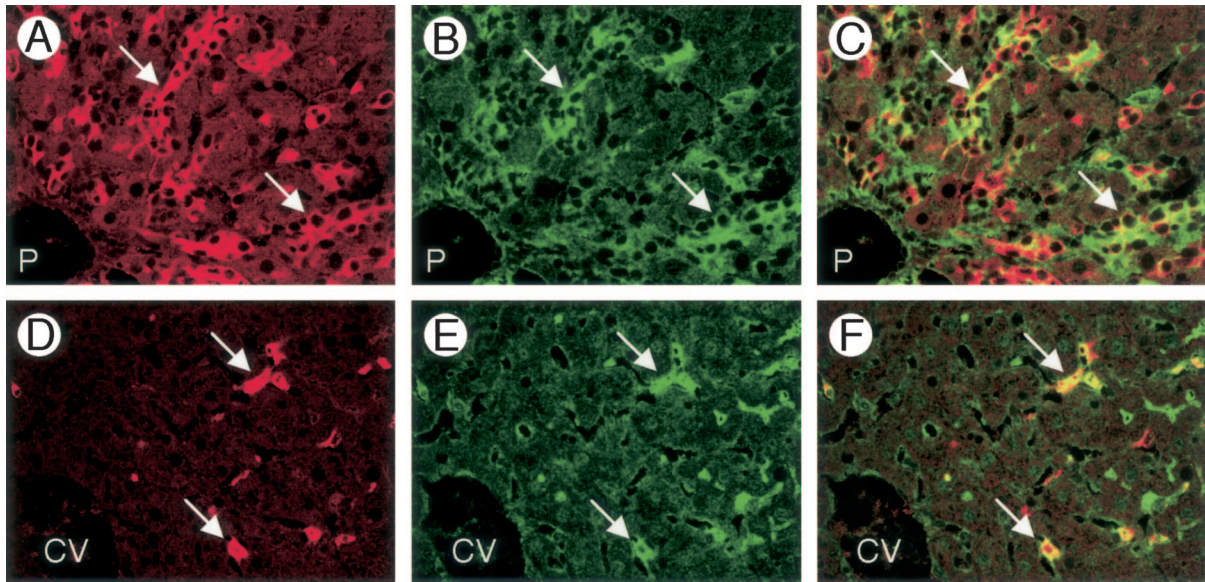


Figure 4. Expression of OSM in the livers in the AAF/PH model. **A:** Fluorescein for CK-19, which is a marker of oval cells (red). **B:** Fluorescein for OSM (green). **C:** Merged confocal image of **A** and **B**. Co-expression of CK-19 and OSM is shown as yellow. **Arrows** indicate representative co-expression of CK-19 and OSM. **D:** Fluorescein for ED2, which is a marker of Kupffer cells (red). **E:** Fluorescein for OSM (green). **F:** Merged confocal image of **D** and **E**. Co-expression of ED2 and OSM is shown as yellow. **Arrows** indicate representative co-expression of ED2 and OSM. **A** to **C** and **D** to **F** are the photographs, demonstrated by confocal laser scanning, of the same section. P, portal vein; CV, central vein.

control conditioned medium were $\sim 10 \mu\text{m}$ in size with a high nuclear to cytoplasmic ratio and ovoid nuclei (Figure 7, A and D). OC15-5 cells cultured with the conditioned medium without OSM were similar in morphology to those cultured with the control conditioned medium (Figure 7, B and E). In contrast, OC15-5 cells cultured with the conditioned medium with OSM were bigger with a decreased nuclear-to-cytoplasmic ratio (Figure 7, C and F). In addition, these OSM-treated OC15-5 cells possessed microvilli on the surface, large cytoplasm with developed organelles including mitochondria, lysosome, and rough endoplasmic reticulum, and clear nucleoli in the nuclei, that were characteristics of hepatocytes (Figure 7; G to I).

Finally, we evaluated the effect of OSM on the expression of markers of oval cells (CK19 and AFP) and hepatocytes (albumin, TAT, and TO) in OC15-5 cells. OC15-5 cells cultured with the control conditioned medium or the conditioned medium without OSM expressed *CK19*, *AFP*, and *albumin* mRNA, but not *TAT* and *TO* mRNA. In contrast, OC15-5 cells cultured with the conditioned medium with OSM expressed *TAT* and *TO* mRNA, higher levels of *albumin* mRNA, and decreased levels of *CK-19* and *AFP* mRNA (Figure 5D). Western blot analysis showed similar changes in CK-19 and albumin expression (Figure 5E). These results indicated that OSM induced the differentiation of OC15-5 cells into hepatocytes.

Abrogation of the Effect by Rat OSM on OC15-5 Cells by siRNA-Mediated Silencing of OSM-R

We introduced an siRNA construct specifically targeting rat OSM-R into OC15-5 cells and examined whether the siRNA-mediated silencing of OSM-R abrogates the effect of the conditioned medium with OSM. Flow cytometry showed that OSM-R expression in OC15-5 cells was abrogated by

the introduction of pRNAT-U6.1/Neo-OSM-R (siRNA), but not pRNAT-U6.1/Neo (vector) (Figure 8A). These results indicated that the introduced construct was active and able to suppress the expression of OSM-R in OC15-5 cells. We then examined the effect of the conditioned medium with OSM on the growth of OC15-5 cells introduced with pRNAT-U6.1/Neo or pRNAT-U6.1/Neo-OSM-R. OC15-5 cells carrying pRNAT-U6.1/Neo-OSM-R (siRNA) markedly proliferated in the presence of the conditioned medium with OSM, whereas OC15-5 cells carrying pRNAT-U6.1/Neo (vector) grew poorly (Figure 8B). Morphologically, OC15-5 cells carrying pRNAT-U6.1/Neo (vector) became bigger with a decreased nuclear to cytoplasmic ratio in the presence of the conditioned medium with OSM. In contrast, OC15-5 cells carrying pRNAT-U6.1/Neo-OSM-R (siRNA) grew with a cobblestone appearance in the presence of the conditioned medium with OSM (Figure 8C).

Finally, we evaluated the effect of the conditioned medium with OSM on the expression of CK-19 and albumin in OC15-5 cells. Western blot analysis showed that OC15-5 cells carrying pRNAT-U6.1/Neo (vector) expressed higher levels of albumin and decreased levels of CK-19 in the presence of the conditioned medium OSM. In contrast, no significant changes of CK-19 and albumin expression were observed in OC15-5 cells carrying pRNAT-U6.1/Neo-OSM-R (siRNA) in the presence of the conditioned medium with OSM (Figure 8D). These results indicated that the effect of the conditioned medium with OSM on OC15-5 cells was abrogated by siRNA-mediated silencing of OSM-R.

Discussion

In this study, we examined whether the OSM/OSM-R system is involved in the differentiation of oval cells into

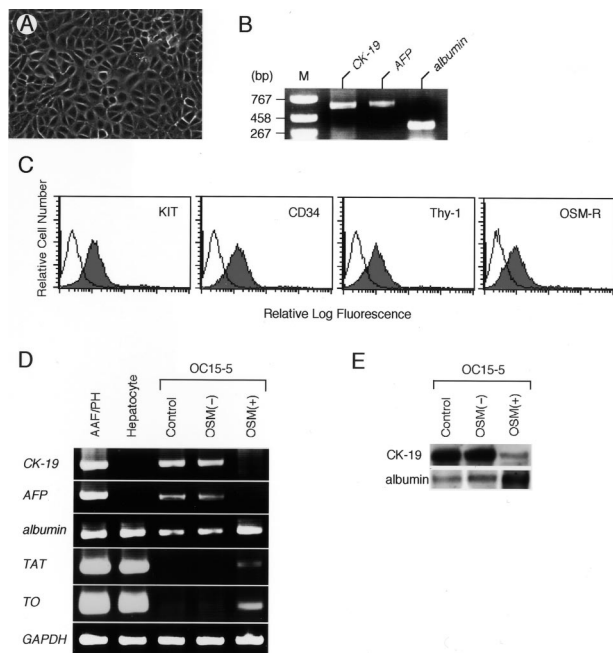


Figure 5. Characterization of OC15-5 cells and effect of OSM on OC15-5 cells. **A:** Phase-contrast microscope. **B:** RT-PCR analysis of *CK-19*, *AFP*, and *albumin* mRNA in OC15-5 cells. Total RNA extracted from OC15-5 cells was reverse-transcribed and PCR-amplified with CK-19, AFP, or albumin primers for 30 cycles. The amplified PCR products were stained with ethidium bromide. M, a size marker. **C:** Flow cytometric analysis of *c-kit* receptor tyrosine kinase (KIT), CD34, Thy-1, and OSM-R expression on the surface of OC15-5 cells. Shaded and open histograms represent staining with anti-*c-kit*, CD34, Thy-1, or OSM-R antibody and rabbit or goat IgG, respectively. **D:** RT-PCR analysis of expression of liver-specific genes in OC15-5 cells. AAF/PH, total RNA isolated from the liver of a rat sacrificed on day 7 after PH in the AAF/PH model, when numerous oval cells were present; Hepatocyte, total RNA from adult liver parenchymal cells; and OC15-5, total RNA from OC15-5 cells, cultured with the control conditioned medium (control), the conditioned medium without OSM [OSM(-)], or the conditioned medium with OSM [OSM(+)] for 4 days. *Glyceraldehyde-3-phosphate dehydrogenase* (*GAPDH*) mRNA was reverse-transcribed and amplified as an internal standard. **E:** Western blot analysis of CK-19 and albumin in OC15-5 cells. Cell lysates from OC15-5 cells, cultured with the control conditioned medium (control), the conditioned medium without OSM [OSM(-)], or the conditioned medium with OSM [OSM(+)] for 4 days, were analyzed. Original magnification, $\times 110$ (A).

hepatocytes, thereby promoting the liver regeneration. First, we isolated the rat *OSM-R* cDNA and, using it as a probe, we conducted time-course analysis of *OSM-R* mRNA in the liver after PH in the AAF/PH model. We found that *OSM-R* mRNA was expressed in a nonparenchymal cell preparation with oval cells and the expression level increased in a good correlation with the increase in the number of oval cells. We then confirmed that oval cells were the sites of expression of *OSM-R* mRNA and OSM-R protein. These results indicate that OSM-R serves as a useful marker for oval cells. Furthermore, in the rat AAF/PH model, we showed that OSM was expressed in the livers on days 7, 9, 11, and 13 after PH and that not only OSM-R but also OSM was expressed in oval cells. Therefore, it is likely that an autocrine signaling of the OSM/OSM-R system participates in the development and differentiation of oval cells. OSM was also found to be expressed in Kupffer cells, consistent with the report of Nakamura and colleagues²⁴ that Kupffer cells are a major source of OSM in the mouse liver injured

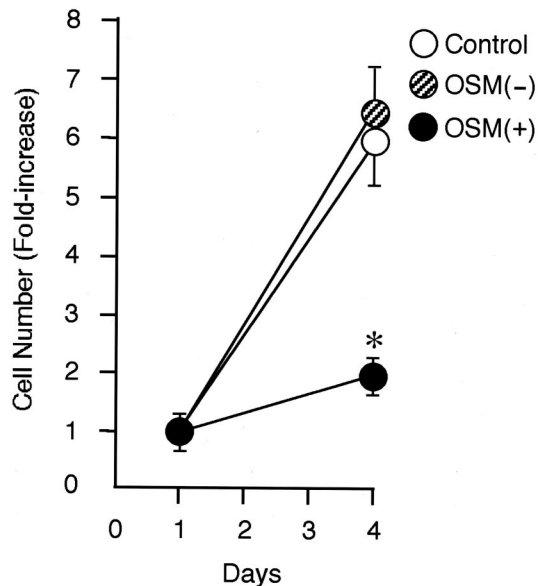


Figure 6. Inhibition of growth of OC15-5 cells by OSM. OC15-5 cells were cultured with the control conditioned medium (control), the conditioned medium without OSM [OSM(-)], or the conditioned medium with OSM [OSM(+)]. After 4 days, the number of viable OC15-5 cells was determined based on the exclusion of trypan blue. The cell number was expressed as fold increases greater than that on day 1. Three independent assays were performed with comparable results, and the values of a representative experiment are shown. Bars are standard errors. Statistically significant differences are indicated by asterisks ($P < 0.05$), when compared with the value of control.

by carbon tetrachloride. There is a possibility that OSM produced by Kupffer cells plays an important role in the liver regeneration.

Next, we isolated the rat *OSM* cDNA and established a rat oval cell line, OC15-5, to study the role of OSM in the differentiation of oval cells. Rat OSM, like mouse and human OSM,^{25,26} contains a predicted signal peptide, four α -helices, and an AB loop. However, it does not contain four positively charged repeats that are present in the C-terminal region of mouse OSM. Previously, Yoshimura and colleagues²⁶ reported that the conditioned medium of COS cells transfected with C-terminally truncated mouse *OSM* cDNA lacking four positively charged repeats exhibited biological activity, but that the conditioned medium of cells transfected with the full-length mouse *OSM* cDNA did not. In this study, we found that the conditioned medium of 293T cells transfected with the full-length rat *OSM* cDNA, in which four positively charged repeats are not present, possessed biological activity. These results indicate that four positively charged repeats interfere with the activity of OSM and that the truncation of C-terminal region carrying four positively charged repeats is essential for the activation of OSM.

OC15-5 cells express not only the traditional oval cell markers (CK-19 and AFP), but also the new oval cell markers (*c-kit* receptor tyrosine kinase, CD34, and Thy-1).¹⁰⁻¹³ OC15-5 cells may be useful to identify the factors that induce the differentiation of oval cells into hepatocytes and study the biological role of oval cells in the liver regeneration. When OC15-5 cells were cultured with the conditioned medium of 293T cells transfected with rat *OSM* cDNA, their growth was suppressed. The morphol-

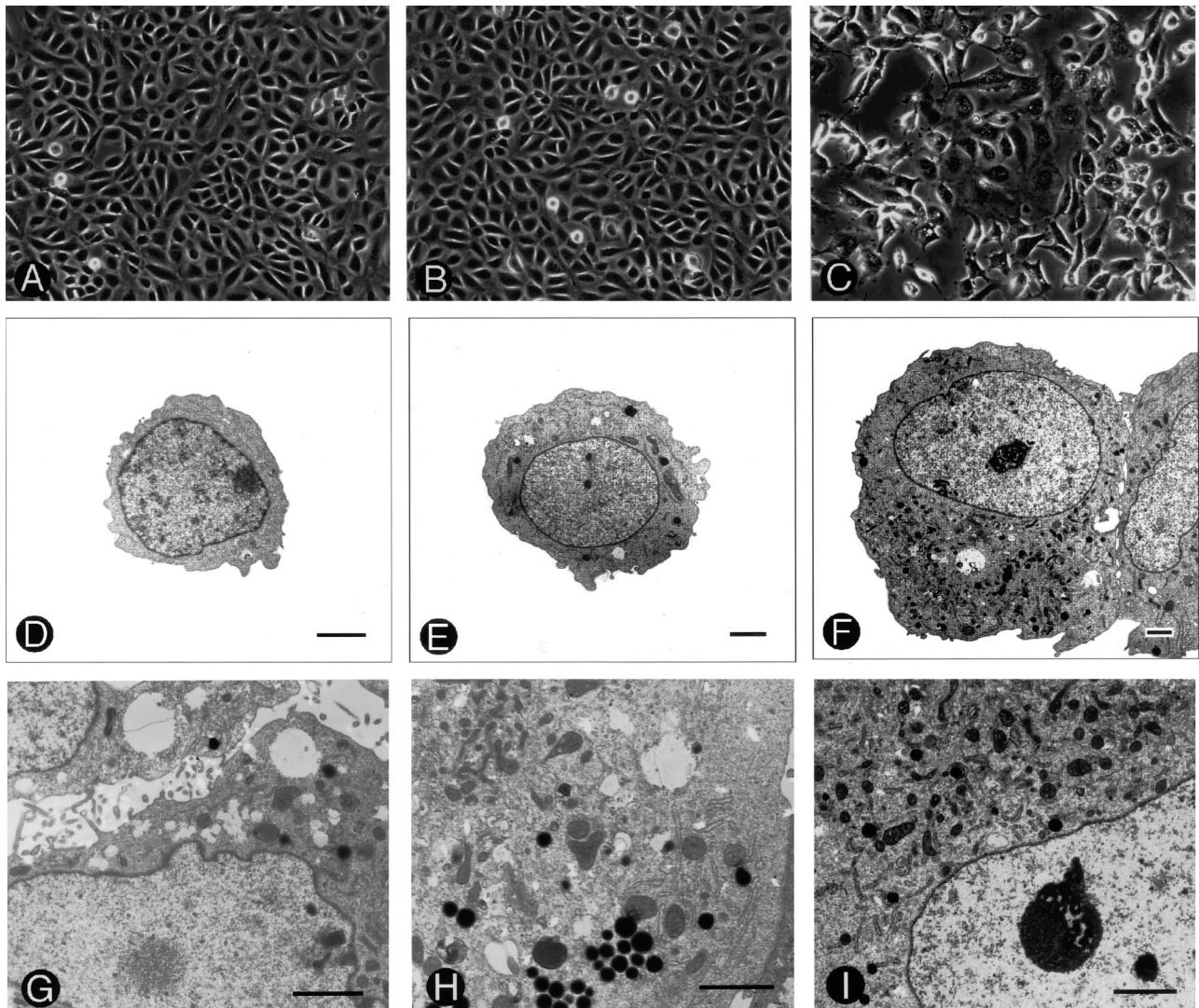


Figure 7. Morphological changes of OC15-5 cells induced by OSM. OC15-5 cells were cultured with the control conditioned medium (**A** and **D**), the conditioned medium without OSM (**B** and **E**), or the conditioned medium with OSM (**C**, **F**, **G**, **H**, and **I**) for 4 days. **A** to **C**: Phase-contrast microscopic analysis. OC15-5 cells, cultured with the control conditioned medium (**A**) and the conditioned medium without OSM (**B**), proliferated with a cobblestone appearance, but OC15-5 cells cultured with the conditioned medium with OSM did not show the cobblestone appearance (**C**). **D** to **I**: Electron microscopic analysis. OC15-5 cells, cultured with the control conditioned medium (**D**) and the conditioned medium without OSM (**E**), exhibited an ovoid nucleus and a high nuclear to cytoplasmic ratio. On the other hand, OC15-5 cells, cultured with the conditioned medium with OSM, became bigger in size (**F**) and showed protruding microvilli on the surface (**G**), large cytoplasm with mitochondria, lysosome, and rough endoplasmic reticulum (**H**), and clear nucleolus in the nucleus (**I**). Scale bars, 2 μ m. Original magnifications, $\times 110$ (**A-C**).

ogy was also changed to become similar to that of hepatocytes. In addition, OC15-5 cells cultured with the conditioned medium with OSM showed decreases in CK-19 and AFP expression, but increases in albumin expression, and were also positive for hepatocyte markers, TAT and TO. These effects of the conditioned medium with OSM were not observed in OC15-5 cells carrying pRNAT-U6.1/Neo-OSM-R, in which OSM-R expression was down-regulated by the introduction of an siRNA construct specifically targeting the rat *OSM-R*. These results indicate that OSM is important for induction of the differentiation of OC15-5 cells into hepatocytes, and suggest that the OSM/OSM-R system plays a pivotal role in oval cell-mediated liver regeneration. We performed similar experiments using primary oval cells isolated from the livers on day 8 after PH in the AAF/PH model. On incubation with

the conditioned medium with OSM, primary oval cells ceased to grow and underwent morphological changes similar to those observed with OC15-5 cells (data not shown). However, analysis of expression of liver-specific proteins by Western blotting could not be performed because of difficulties of obtaining primary oval cells in sufficient quantities. These results, although limited, supported the conclusion derived from OC15-5 cells.

Previously, Kamiya and colleagues¹⁸ demonstrated that OSM in combination with glucocorticoid induces differentiation of fetal hepatocytes to express TAT and glucose-6-phosphatase, which are expressed in the perinatal liver. However, no adult liver-specific enzymes, such as TO, were expressed in these cells. These results suggest that OSM renders the characteristics of the neonatal liver, but not of adult hepatocytes, to fetal hepatocytes. In

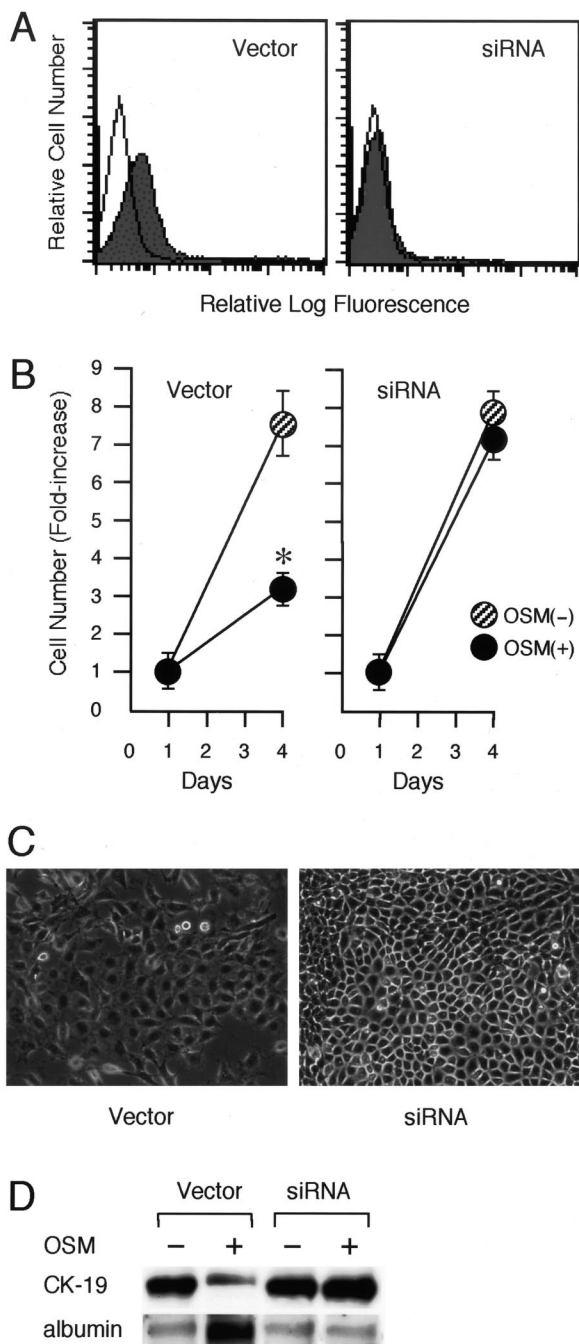


Figure 8. Suppression of OSM-induced growth inhibition and differentiation of OC15-5 cells by siRNA for *OSM-R*. **A:** Flow cytometric analysis of OSM-R expression on the surface of OC15-5 cells introduced with pRNAT-U6.1/Neo (vector) or pRNAT-U6.1/Neo-OSM-R (siRNA). **Shaded and open histograms** represent staining with anti-OSM-R antibody and goat IgG, respectively. **B:** Cell growth. OC15-5 cells introduced with pRNAT-U6.1/Neo (vector) or pRNAT-U6.1/Neo-OSM-R (siRNA) were cultured with the conditioned medium without OSM [OSM(-)] or the conditioned medium with OSM [OSM(+)]. After 4 days, the number of viable cells was determined based on the exclusion of trypan blue. The cell number was expressed as fold-increase greater than that on day 1. Three independent assays were performed with comparable results, and the values of a representative experiment are shown. Bars are standard errors. Statistically significant differences are indicated by **asterisks** ($P < 0.05$), when compared with the value of OSM(-). **C:** Phase-contrast microscopic analysis of OC15-5 cells introduced with pRNAT-U6.1/Neo (vector) or pRNAT-U6.1/Neo-OSM-R (siRNA) cultured with the conditioned medium with OSM for 4 days. **D:** Western blot analysis of cell lysates from OC15-5 cells introduced with pRNAT-U6.1/Neo (vector) or pRNAT-U6.1/Neo-OSM-R (siRNA) cultured with the conditioned medium with or without OSM for 4 days. Original magnification, $\times 60$ (C).

this study, *TO* mRNA expression was induced in OC15-5 cells by culturing with the conditioned medium of 293T cells transfected with rat *OSM* cDNA. Several possibilities may be raised to explain the difference between the results of Kamiya and colleagues¹⁸ and ours. First, OSM-R-mediated signal transduction is sufficient for the differentiation of oval cells into adult hepatocytes, but not for the maturation of fetal hepatocytes. Second, OSM may induce the maturation of OC15-5, an oval cell line, but not primary oval cells, into adult hepatocytes. Third, 293T cells produce soluble factors required for full maturation of oval cells. This idea is supported by the findings that fetal hepatocytes on embryonic day 14.5 are induced to express *TO* mRNA by culturing with OSM and extracellular matrices derived from Engelbreth-Holm-Swarm sarcoma.¹⁹

Both OSM and hepatocyte growth factor (HGF) are involved in the maturation of fetal hepatocytes.^{28,29} The OSM-induced hepatic maturation is inhibited by the expression of a dominant-negative form of signal transducer and activator of transcription protein 3, whereas HGF-induced hepatic maturation is not, indicating that OSM and HGF induce the maturation of fetal hepatocytes through different signaling pathways.²⁸ As for the effect on the oval cells, Okano and colleagues³⁰ reported that HGF induces the proliferation of oval cells through the phosphatidylinositol-3 kinase/Akt signaling pathway, and Shiota and colleagues³¹ reported that HGF accelerates the proliferation of oval cells in the AAF/PH model. On the other hand, the present study showed that OSM induces the differentiation of oval cells into hepatocytes. These results suggest that a combined use of HGF and OSM, that support the proliferation and differentiation of oval cells, respectively, may be of value for the treatment of patients with liver damages.

Acknowledgments

We thank Dr. Tetsu Hayakawa of Hyogo College of Medicine (Nishinomiya, Hyogo, Japan) for his valuable advice; and Ms. Michiko Kakihana, Ms. Hatsuka Seki, Mr. Kunihisa Hamada, Mr. Hirotsugu Kubo, and Mr. Masahito Yagi of Hyogo College of Medicine for their technical assistance.

References

- Steer CJ: Liver regeneration. *FASEB J* 1995, 9:1396-1400
- Sell S: Heterogeneity and plasticity of hepatocyte lineage cells. *Hepatology* 2001, 33:738-750
- Fausto N, Campbell JS: The role of hepatocytes and oval cells in liver regeneration and repopulation. *Mech Dev* 2003, 120:117-130
- Farber E: Similarities in the sequence of early histological changes induced in the liver of the rat by ethionine, 2-acetylaminofluorene, and 3'-methyl-4-dimethylaminoazobenzene. *Cancer Res* 1956, 16:142-148
- Grisham JW, Thorgerirsson SS: Liver stem cells. *Stem Cells*. Edited by Potten CS. London, Academic Press, 1997, pp 233-282
- Oh SH, Hatch HM, Petersen BE: Hepatic oval 'stem' cell in liver regeneration. *Semin Cell Dev Biol* 2002, 13:405-409
- Alison MR, Vig P, Russo F, Bigger BW, Amofah E, Themis M, Forbes

- S: Hepatic stem cells: from inside and outside the liver? *Cell Prolif* 2004, 37:1–21
8. Thorgeirsson SS, Grisham JW: Overview of recent experimental studies on liver stem cells. *Semin Liver Dis* 2003, 23:303–312
 9. Everts RP, Nagy P, Marsden E, Thorgeirsson SS: A precursor-product relationship exists between oval cells and hepatocytes in rat liver. *Carcinogenesis* 1987, 8:1737–1740
 10. Fujio K, Everts RP, Hu Z, Marsden ER, Thorgeirsson SS: Expression of stem cell factor and its receptor, c-kit, during liver regeneration from putative stem cells in adult rat. *Lab Invest* 1994, 70:511–516
 11. Matsusaka S, Tsujimura T, Toyosaka A, Nakasho K, Sugihara A, Okamoto E, Uematsu K, Terada N: Role of c-kit receptor tyrosine kinase in development of oval cells in the rat 2-acetylaminofluorene/partial hepatectomy model. *Hepatology* 1999, 29:670–676
 12. Omori N, Omori M, Everts RP, Teramoto T, Miller MJ, Hoang TN, Thorgeirsson SS: Partial cloning of rat CD34 cDNA and expression during stem cell-dependent liver regeneration in the adult rat. *Hepatology* 1997, 26:720–727
 13. Petersen BE, Goff JP, Greenberger JS, Michalopoulos GK: Hepatic oval cells express the hematopoietic stem cell marker Thy-1 in the rat. *Hepatology* 1998, 27:433–445
 14. Gomez-Lechon MJ: Oncostatin M: signal transduction and biological activity. *Life Sci* 1999, 65:2019–2030
 15. Taga T, Kishimoto T: Gp130 and the interleukin-6 family of cytokines. *Annu Rev Immunol* 1997, 15:797–819
 16. Miyajima A, Kinoshita T, Tanaka M, Kamiya A, Mukoyama Y, Hara T: Role of oncostatin M in hematopoiesis and liver development. *Cytokine Growth Factor Rev* 2000, 11:177–183
 17. Tanaka M, Hara T, Copeland NG, Gilbert DJ, Jenkins NA, Miyajima A: Reconstitution of the functional mouse oncostatin M (OSM) receptor: molecular cloning of the mouse OSM receptor β subunit. *Blood* 1999, 93:804–815
 18. Kamiya A, Kinoshita T, Ito Y, Matsui T, Morikawa Y, Senba E, Nakashima K, Taga T, Yoshida K, Kishimoto T, Miyajima A: Fetal liver development requires a paracrine action of oncostatin M through the gp130 signal transducer. *EMBO J* 1999, 18:2127–2136
 19. Kamiya A, Kojima N, Kinoshita T, Sakai Y, Miyajima A: Maturation of fetal hepatocytes in vitro by extracellular matrices and oncostatin M: induction of tryptophan oxygenase. *Hepatology* 2002, 35:1351–1359
 20. Lázaro CA, Croager EJ, Mitchell C, Campbell JS, Yu C, Foraker J, Rhim JA, Yeoh GC, Fausto N: Establishment, characterization, and long-term maintenance of cultures of human fetal hepatocytes. *Hepatology* 2003, 38:1095–1106
 21. Shimano K, Satake M, Okaya A, Kitanaka J, Kitanaka N, Takemura M, Sakagami M, Terada N, Tsujimura T: Hepatic oval cells have the side population phenotype defined by expression of ATP-binding cassette transporter ABCG2/BCRP1. *Am J Pathol* 2003, 163:3–9
 22. Tsujimura T, Furitsu T, Morimoto M, Isozaki K, Nomura S, Matsuzawa Y, Kitamura Y, Kanakura Y: Ligand-independent activation of c-kit receptor tyrosine kinase in a murine mastocytoma cell line P-815 generated by a point mutation. *Blood* 1994, 83:2619–2626
 23. Mosley B, De Imus C, Friend D, Boiani N, Thoma B, Park LS, Cosman D: Dual oncostatin M (OSM) receptors. Cloning and characterization of an alternative signaling subunit conferring OSM-specific receptor activation. *J Biol Chem* 1996, 271:32635–32643
 24. Nakamura K, Nonaka H, Saito H, Tanaka M, Miyajima A: Hepatocyte proliferation and tissue remodeling is impaired after liver injury in oncostatin M receptor knockout mice. *Hepatology* 2004, 39:635–644
 25. Malik N, Kallestad JC, Gunderson NL, Austin SD, Neubauer MG, Ochs V, Marquardt H, Zurling JM, Shoyab M, Wei C-M, Linsley PS, Rose TM: Molecular cloning, sequence analysis, and functional expression of a novel growth regulator, oncostatin M. *Mol Cell Biol* 1989, 9:2847–2853
 26. Yoshimura A, Ichihara M, Kinjyo I, Moriyama M, Copeland NG, Gilbert DJ, Jenkins NA, Hara T, Miyajima A: Mouse oncostatin M: an immediate early gene induced by multiple cytokines through the JAK-STAT5 pathway. *EMBO J* 1996, 15:1055–1063
 27. Yasui O, Miura N, Terada K, Kawarada Y, Koyama K, Sugiyama T: Isolation of oval cells from Long-Evans Cinnamon rats and their transformation into hepatocytes in vivo in the rat liver. *Hepatology* 1997, 25:329–334
 28. Ito Y, Matsui T, Kamiya A, Kinoshita T, Miyajima A: Retroviral gene transfer of signaling molecules into murine fetal hepatocytes defines distinct roles for the STAT3 and ras pathways during hepatic development. *Hepatology* 2000, 32:1370–1376
 29. Kamiya A, Kinoshita T, Miyajima A: Oncostatin M and hepatocyte growth factor induce hepatic maturation via distinct signaling pathways. *FEBS Lett* 2001, 492:90–94
 30. Okano J, Shiota G, Matsumoto K, Yasui S, Kurimasa A, Hisatome I, Steinberg P, Murawaki Y: Hepatocyte growth factor exerts a proliferative effect on oval cells through the PI3K/AKT signaling pathway. *Biochem Biophys Res Commun* 2003, 309:298–304
 31. Shiota G, Kunisada T, Oyama K, Udagawa A, Nomi T, Tanaka K, Tsutsumi A, Isono M, Nakamura T, Hamada H, Sakatani T, Sell S, Sato K, Ito H, Kawasaki H: In vivo transfer of hepatocyte growth factor gene accelerates proliferation of hepatic oval cells in a 2-acetylaminofluorene/partial hepatectomy model in rats. *FEBS Lett* 2000, 470:325–330